Supplementary information for

Randomness in the choice of neighbours promotes cohesion in mobile animal groups

Vivek Jadhav, Vishwesha Guttal and Danny Raj M

December 6, 2021

1 Some comments on the asynchronous and probabilistic nature of interactions

The model we present (section II of main text) is a non-trivial extension of the mean-field model developed by Jhawar et al. 2020: *inclusion of space and variable speed*. Similar to other agent-based models employed in this field, agents align with their neighbours and attract to them. Individuals also maintain a minimum distance with their neighbours to avoid collision and also turn spontaneously (Huth and Wissel 1992, Huth and Wissel 1994, Couzin et al. 2002, Hemelrijk and Kunz 2005, Hemelrijk and Hildenbrandt 2008, Jhawar et al. 2020).

The distinct features of our model are that interactions are,

1. **probabilistic**: modelled as independent stochastic events, owing to the inherently probabilistic nature of animal interactions and
2. **asynchronous**: every fish interacts via one kind of interaction, at a randomly chosen time.

While some models in literature have some of the above features, there is none that incorporates all of them simultaneously.

The speed and direction of individuals in the school change due to the following reasons: *i*) **interactions and reactions** independently change the speed and direction of motion of the agents stochastically; *ii*) **collision avoidance**—agents slow down and change direction when they encounter another agent. This appears as a course-correction term to the agent's instantaneous velocity.

We use continuous-time Gillespie simulation (Gillespie 1976, Gillespie 1977) to model the stochastic attraction, spontaneous turning and alignment events for every agent. The time for an event (a particular interaction) for a given agent is sampled from an exponential distribution with mean corresponding to the rate of that interaction. This ensures that the time of the event is independent of the agent's past interactions. Note, that while the velocity of the agents change only as interaction events happen, the positions of the agents are updated at every time step in a regular fashion.

Fish avoid collisions by adjusting their speed and orientation with respect to neighbours (observed by Katz et al. 2011, Herbert-Read et al. 2011, Lei et al. 2020). In typical computational models, speed is either a constant or independent of its neighbours. In our model, speed–change during an interaction depends on the state of the agent and its neighbours in the following ways: *i*) when an agent is attracted to an agent far away, it moves faster; *ii*) an agent copies the speed while copying the direction during alignment.

2 Sensitivity to parameter values

The range parameter values explored in the study are given in (Table.1).

Parameter	Unit	Symbol	Value(s) explored
Spontaneous rate	s^{-1}	r_s	0.1-5.0
Alignment rate	s^{-1}	r_p	0.15-10
Attraction rate	s^{-1}	r_a	0.1-10
Visual Field	Degree	θ_s	$90^0 - 360^0$
Desired Speed	$cm\, s^{-1}$	s_0	0.2 - 1
Maximum Speed	$cm\, s^{-1}$	s_{max}	$5 \times s_0$
Agent size	cm	R	0.2
Variance of angular displacement (spontaneous turn)	rad^2	σ_a	$\frac{\theta_s \times \pi}{2 \times 180}$
Variance of speed (spontaneous turn)	$cm^2\, s^{-2}$	σ_s	s_0
Relaxation time for speed	s	τ	0.2
Relaxation time for angular speed	s	τ_θ	0.5
Distance-dependent attraction (coefficient)	$cm\, s^{-1}$	κ_a	10^{-2} - 1
Distance-dependent attraction (order)	1	γ	3-10
Zone of repulsion	cm	zor	1.2
Distance-dependent repulsion (coefficient)	cm^β	κ_r	-10^{-3} - -1
Distance-dependent repulsion (order)	1	β	3-10
Maximum distance between agents to belong to the same cluster	cm	ϵ	zor - $3 \times zor$

Table 1: Summary of model parameters.

In this section, we show that the qualitative features of our primary result (cohesion parameter as a function of the topological neighbourhood; figure 2b in main text) is robust to changes in parameters in the model. Throughout the SI text, unless mentioned same parameter values reported in the main text are used and the group size is set to 30.

We begin by varying the parameters determining the strength of attraction and repulsion (κ_a, κ_r, β, and γ). We find that the cohesion parameter ($\mathcal{C}$) does not change qualitatively (figure 1).

Effect of β, γ, κ_r and κ_a

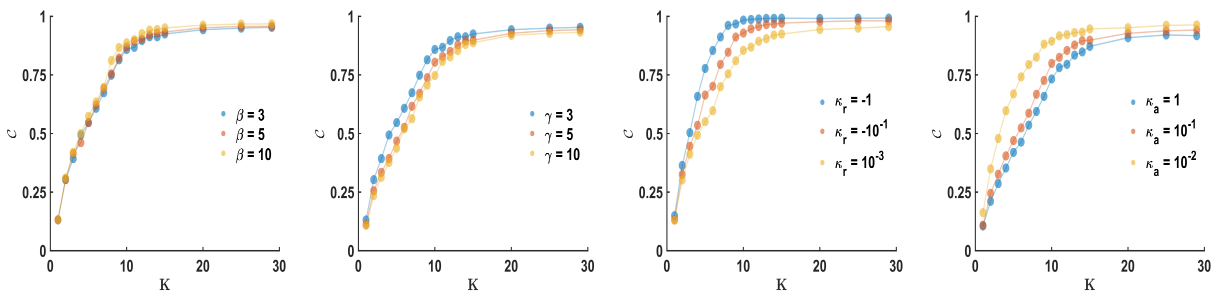

(a) Effect of β (b) Effect of γ (c) Effect of κ_r (d) Effect of κ_a

Figure 1: Cohesion parameter $\mathcal{C}$ depends on the topological neighbourhood K in a qualitatively similar manner (like in figure 2B of main text) across a range of parameters that describe how attraction/repulsion are implemented.

Next, we vary the interaction rates (alignment, attraction) on the schooling dynamics, one at a time while keeping the other constant.

We first vary the attraction rates from 0.1 events per second to 10 events per second. When the attraction rate (r_a) is very low (~ 0.1 s^{-1}), the group fails to be cohesive for all values of K (2a). This is not surprising given that attraction interaction is central to the group-cohesion. When attraction rates are low, agents do not interact with sufficient number of neighbours within a given time. Consequently, the group breaks into smaller clusters and do not stay cohesive. As the attraction rate (r_a) increases, the groups are cohesive, and the K required to achieve a similar cohesion parameter decreases with an increase in attraction rates (figure 2a).

Second, we vary the alignment interaction rates in a similar manner. Although alignment stand-alone cannot ensure group cohesion (Section 4), along with attraction interaction, higher alignment rates give rise to higher cohesivities (figure 2b).

Third, we vary the desired speed of the agents from 0.1 to 1. We find that agents escape the group, often, resulting in lesser cohesivity (figure 2c).

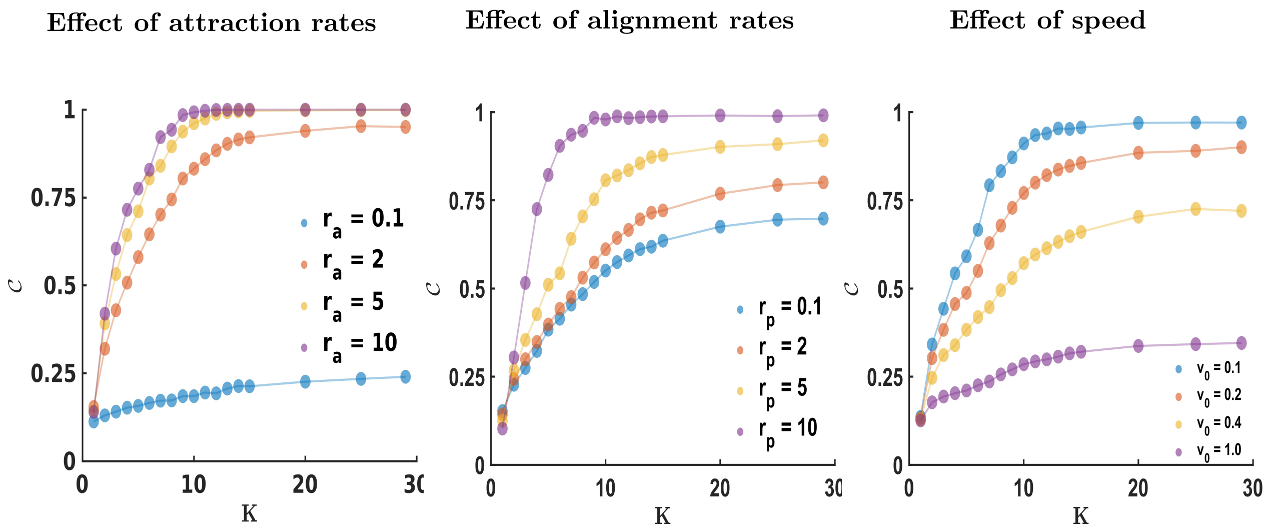

(a) (b) (c)

Figure 2: Cohesion parameter $\mathcal{C}$ vs topological neighbourhood K trends observed across a range of interaction rates and average speeds are found to have the same qualitative features as figure 2B of main text. (a) We observe that Cohesion Parameter $\mathcal{C}$ increases with an increase in attraction rate r_a for fixed values of alignment and spontaneous interactions, 0.5 s^{-1} and 1.5 s^{-1} respectively. (b) Alignment rates facilitate group cohesion in presence of attraction interaction. $r_s = 1.0\ \mathrm{s}^{-1}$ and $r_a = 0.5\ \mathrm{s}^{-1}$. (c) Cohesion Parameter ($\mathcal{C}$) decreases with the average speed of agents as agents in the group move apart easily.

Next, we study the effect of the size of the visual field of the agents on cohesion. When the visual field is too narrow, the agents fail to be cohesive. As the sight increases, the groups become more and more cohesive (figure 3a). However, we do not observe any monotonic increase in cohesion with an increase in visual field. Also, for higher visual fields (sight $> 300^0$), larger K is required to achieve the same cohesion as that achieved for lower visual fields ($210^0 <$ sight $< 270^0$). However, note that the qualitative features of $\mathcal{C}$ vs K are similar across the broad range of visual fields.

Further, to check the generality of our findings, we also modify our model by removing its key components like its probabilistic nature of the interaction, i.e., in this case, an agent interacts via all three types of interactions (alignment, attraction and spontaneous change) simultaneously. However, the time for an agent to interact is still chosen stochastically, and different agents interact at different times. In a second variant of the model, all the agents interact via all the interactions simultaneously. Nevertheless, the time chosen for agents to interact is still chosen stochastically with a constant rate. We call these models Model-1 and Model-2, respectively. In both cases, we find that the results do not change qualitatively (figure 3b). However, these non-probabilistic and semi-synchronous models result in more cohesive groups than the model discussed in the main text.

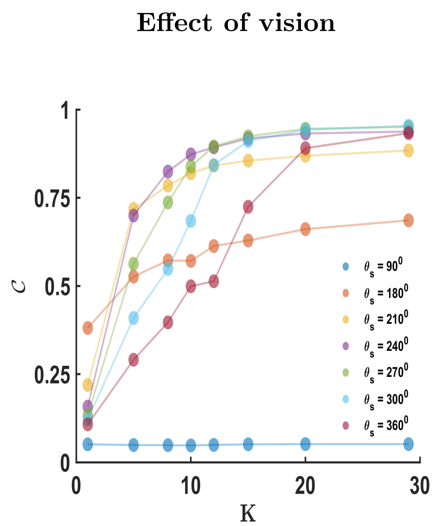

(a)

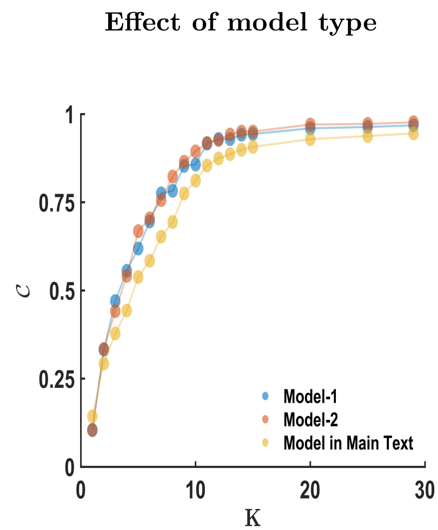

(b)

Figure 3: Cohesion parameter $\mathcal{C}$ vs topological neighbourhood K trends observed across different values of agent-vision and the different variants of the model are found to have the same qualitative features as figure 2B of main text. (a) Cohesion Parameter ($\mathcal{C}$) is negligible for narrow visual angle and increases when agents have a wide visual angle. (b) Variants of Model-1 and Model-2 yield similar results as the original. We also find these semi-synchronous models to give rise to slightly more cohesive groups than the model discussed in the main text.

We also investigate an alternate method to quantify group cohesion to ensure that the study is not sensitive to the choice of the order parameter. Cohesion parameter in this case $\mathcal{C}_t$ is defined as the fraction of time the group was cohesive during the simulation. Isolated agents are treated as 'noise'. Only when a pair or more break away from the group, it is considered non-cohesive. For example, if a group of size 4 breaks into sub-groups of sizes 1 and 3, we consider it a single cluster and therefore cohesive according to this definition. For this definition of cohesion parameter ($\mathcal{C}_t$), we observe that $\mathcal{C}_t$ is close to zero till a critical K after which $\mathcal{C}_t$ increases non-linearly (figure 4a). Here, we want to emphasise that even if just two agents out of 50 break away from the group, we say the group is not cohesive for this definition of cohesion parameter. However, the broad features of $\mathcal{C}_t$ vs K are qualitatively similar to that of $\mathcal{C}$ vs K reported in figure 2b of main text.

We also compare if the cohesion parameter ($\mathcal{C}_p$) defined in the main text depends on the choice of ϵ. The results are qualitatively similar independent of ϵ (figure 4b). For very small values of ϵ, it appears as if the group is not cohesive. This is mainly because, within this distance, i.e., $\epsilon \leq zor$, the agents are trying to move away from each other. However, this does not imply that the group is not cohesive.

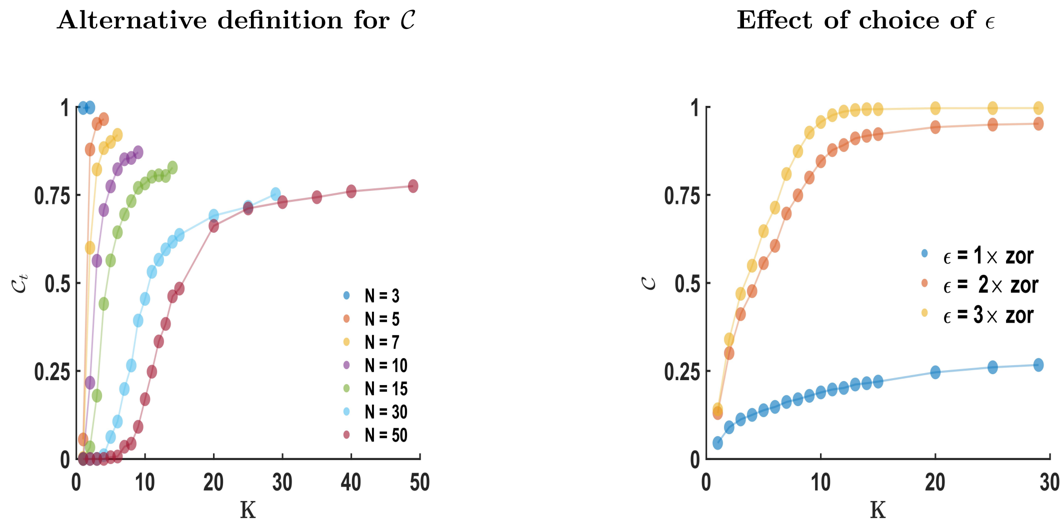

(a) (b)

Figure 4: (a) Alternate metric to quantify cohesion ($\mathcal{C}_t$), based on the fraction of time the group was cohesive, plotted for different group sizes. For large group sizes, $\mathcal{C}_t$ is found to be close to zero till a critical K after which $\mathcal{C}_t$ increases rapidly. (b) Cohesion Parameter ($\mathcal{C}$), as defined in the main text section 2, evaluated for different values of ϵ show that the qualitative features of $\mathcal{C}$ vs K remain the same.

In the main text, while discussing results, we state that the cohesion parameter saturates as the ratio of the topological neighbourhood to the total group size approaches 0.3. However, it is important to note that this ratio decreases for higher interaction rates, r_a and r_p (figure 5a and 5b), and lower speeds (figure 5c). For very high attraction rates (for example, $r_a = 10$ s^{-1}), the agents interact many times with neighbours with a given time window (t_w). This ensures a dense interaction network even for small K. Hence, the topological neighbourhood required to achieve cohesive groups reduces for high interaction rates (figure 5a). Thus reducing the ratio discussed in the main text. Similarly, when the alignment rates are very high (for example, $r_a = 10$ s^{-1}), the agents mostly tend to move in the direction of their neighbours. Hence, in this case, interacting with fewer neighbours, even for a low attraction rate, ensures group cohesion (figure 5b). We have also discussed that in the presence of attraction interaction, alignment interaction facilitates group cohesion. A similar trend is observed when we reduce the speed of agents. As the agents move slowly, it takes them a lot of time to move away from each other. Attraction interaction with fewer topological neighbours within this time interval suffices to bring the agents back together (figure 5c).

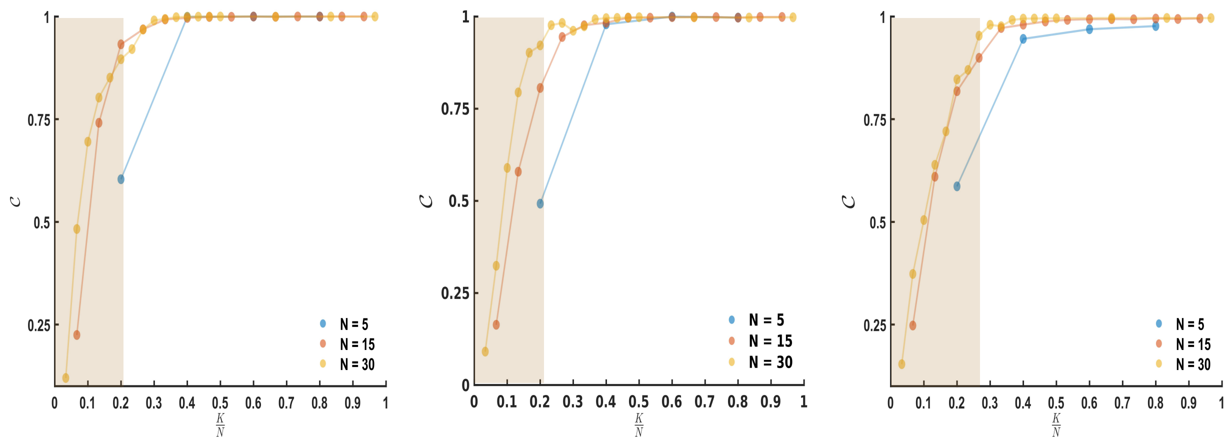

(a) (b) (c)

Figure 5: The threshold ratio ($\frac{K}{N}$) at which cohesion parameter saturates, decreases as interaction rates increases or speed decreases. (a) - Higher attraction rates at $r_a = 10$ s^{-1}, (b) - Higher alignment rates at $r_p = 10$ s^{-1}, and (c) Lower movement speeds at $s_0 = 0.05$cms^{-1}. Except the specific parameter that was changed, the others were set to: $r_s = 1$ s^{-1}, $r_p = 1.5$ s^{-1}, $r_a = 1$ s^{-1} and $s_0 = 0.2$cm s^{-1}.
.

3 Attraction interaction with unique neighbours

We calculate the number of unique neighbours an agent interacts with, to understand the effect of K on cohesion. We construct graph $\mathcal{G}$ as discussed in the main text, Appendix B. We then compute *out-degree* for each node in $\mathcal{G}$, i.e., number of neighbours node i was attracted to. We find the average number of unique neighbours an agent is attracted to within a time window, t_w increases with K. Therefore, for smaller K, particularly when $K = 1$, agents interact with the same neighbour in the time window over which the network was constructed.

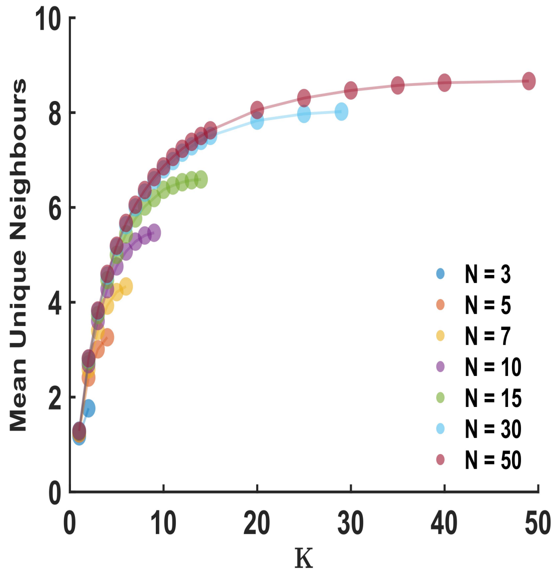

Figure 6: The average number of unique neighbours an agent interacts with increases rapidly with K for all group sizes.

4 Attraction interaction networks are sufficient to characterize cohesion

It is well known that both attraction and alignment interactions affect group cohesion. While attraction interaction brings the agents close to each other, alignment interaction ensures that agents do not move in directions independent of other agents. Hence, to understand which of these interactions one should use to construct the network, we explore which of the contributions of these social interactions to cohesion.

To understand the role of attraction, we set the rate of alignment to zero. This ensures that any group cohesion observed in our simulation is because of the attraction interactions and not alignment. We then calculate the cohesion parameter ($\mathcal{C}$) as a function of K. Similarly, to study the effect of alignment on cohesion, we set the attraction rate to zero.

Figure 7 shows how $\mathcal{C}$ varies with K for these two cases. We see that attraction interactions achieve high levels of group cohesion, while alignment alone cannot ensure group cohesion. We would like to reiterate that our simulations are in an unbounded domain, where agents can drift apart even if they are moving in approximately the same direction. Therefore, we conclude that it is sufficient to look at attraction interactions to understand the emergence of cohesion in groups. However, it is essential to note that alignment interactions can facilitate cohesion in the presence of attraction interactions, changing $\mathcal{C}$ quantitatively (figure 2b).

Though alignment interactions alone cannot increase group cohesion, attraction interactions are found to give rise to significant group polarisation (inset of figure 7). Polarisation is defined as $\frac{1}{N}|\sum_i \frac{\mathbf{v}_i}{v_i}|$, where $\mathbf{v}_i$ is velocity of agent i and v_i is its speed. This is in line with the findings of Strömbom et al. 2019, who argue that asynchronous attraction interactions can give rise to cohesion.

Nevertheless, it is important to note that these results for simulation time $T = 3500s$ are for low alignment rates. For very high alignment rates ($r_p > 10\ \mathrm{s}^{-1}$), as all the agents move in the same direction because of high rates of alignment and little stochasticity ($r_s = 1\ \mathrm{s}^{-1}$), it takes a very long time for them to diffuse apart, but they diffuse eventually. So, even for very high alignment rates if we carry out simulations for very long times ($T > 10000s$) the agents fail to stay cohesive.

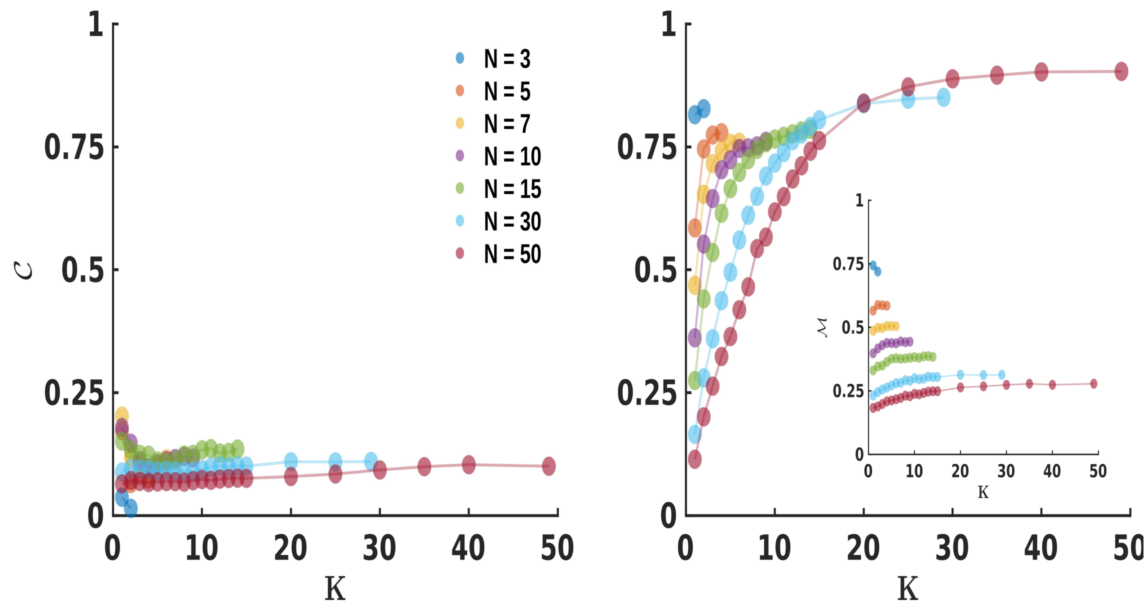

Figure 7: Group cohesion due to alignment interaction alone without any attraction interaction and *vice versa* are explored. (a) With only alignment, the group is not cohesive for all values of K for all group sizes N. (b) With only attraction, groups of all sizes are found to be cohesive (with increasing K) irrespective of the low values of group polarisation (see inset), which shows that attraction interactions play a crucial role in group cohesion in unbounded pairwise interacting systems.

5 Attraction interaction network analysis is consistent across parameters

We show that the network analysis works well across different trends observed in group cohesion. We compute network parameter ($\mathcal{N}_p$) for various parameters where the group cohesion is minimal (low sight angle), intermediate (for high cruise speed or) and very high (high attraction and alignment rates). When the sight angle is low (180^0), the agents are unable to 'see' their neighbours, consequently unable to interact with them, which can be seen through the measure of network parameter. Therefore, irrespective of the neighbours, the agents can perceive they cannot stay cohesive (figure 8a).

When the cruise speed is high ($s_0 = 1\mathrm{cm\,s}^{-1}$), even though the agents interact with their neighbours through attraction, they quickly move away because of spontaneous interaction or interaction with other far away neighbours. The agents are unable to form 'well connected' networks, therefore, failing to achieve high group cohesion (figure 8b), and we only observe intermediate levels of cohesion.

We also consider the case where attraction (and alignment) rates are very high ($r_a = 20\ \mathrm{s}^{-1}$). In this case, the agents interact with large number of neighbours with in a give time, hence resulting in dense interaction network and therefore very high group cohesion (figure 8c). As discussed in section 4, alignment interactions too facilitate cohesion in presence of attraction interaction. So, as the alignment rates are very high in this case ($r_p = 20\ \mathrm{s}^{-1}$), we see that in figure 8c for lower K's, $\mathcal{C} < \mathcal{N}_p$ as we don't account for alignment interaction network in network analysis.

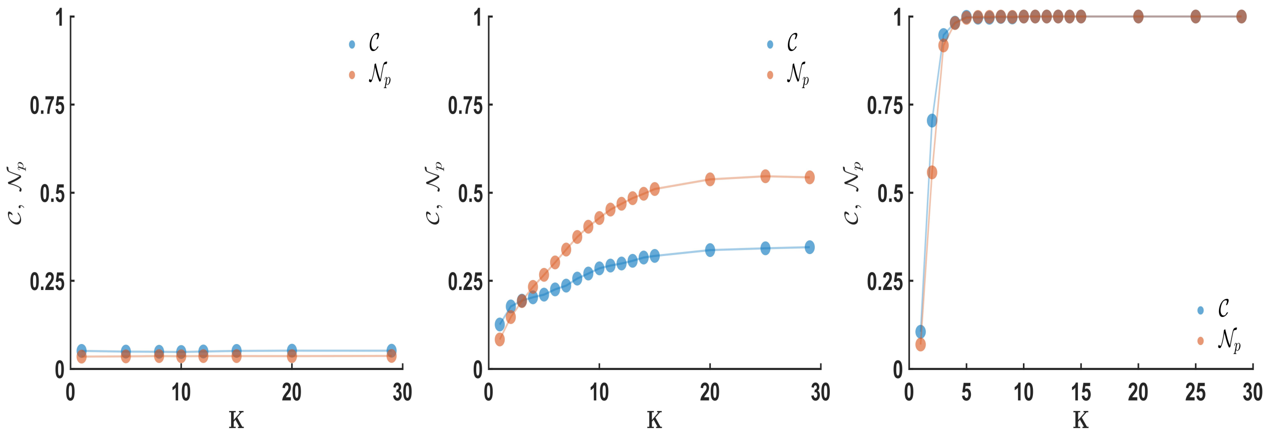

(a) (b) (c)

Figure 8: Network parameter $\mathcal{N}_p$ is found to have the same qualitative features as $\mathcal{C}$ with topological neighbourhood K, for a variety of different group cohesivities. (a) - Case where group cohesion is very low for all K (achieved by setting a narrow vision for agents); (b) - Case where group cohesion is intermediate (by setting a high average speed); (c) - Case where group cohesion is very high (by setting very high for high attraction and alignment rates).

Span shots of networks constructed over consecutive time windows are given in figure 9a and 9b. In figure 9a and 9b circular dots represents the heading of agents in 2-D space. The neighbours they were attracted to within the time window t_w are shown through blue arrows. The direction of the blue arrow indicates the direction of attraction interaction. As defined in section III of the main text, agents belonging to the same sub-group are marked with the same colour. Agents belonging to the same cluster is also shown.

For, high attraction rates ($r_a > 0.5$ s^{-1}) and large K's ($K > 0.3N$, for the parameters used in the main text), we see that the network is dense with network parameter, $\mathcal{N}_p = 0.9$ and cohesion parameter, $\mathcal{C} = 0.9$. We observe that whenever the network is 'well-connected', the agents tend to stay cohesive for longer times (figure 9a). And, even if they break apart the network ensures that they won't drift apart.

For, low attraction rates or $K = 1$ (in figure 9b), the agents form a cluster of size 2-6 for $N = 10$ at some instances of time as they are attracted towards each other. For example, agents 1,2,3,5,7 and 8 in the figure 9b form a cluster, therefore resulting in $\mathcal{C}_p = 0.6$. However, the network is not 'well connected' as the interactions are only from one side. For example, agents 1 and 3 do not interact with 5 or 8; therefore, the cluster can break apart easily as all the agents are not interacting with all the other agents directly or indirectly — as observed in figure 9b ($\mathcal{N}_p = 0.2$ in this case). Consequently, we observe $\mathcal{C} > \mathcal{N}_p$ and $\mathcal{C}, \mathcal{N}_p << 1$ for these values. Hence, we observe low group cohesion for low attraction rates and small K.

Therefore, it is important to note that when the attraction rates are very low or $K = 1$ for higher N, the agents are partly cohesive, but the interactions are sparse; hence the network is not fully connected. As the agents do not form a 'well connected' network, they break apart often. Therefore, low group cohesion. Hence, we argue that it is crucial to forming a 'well-connected' network to achieve a large cohesion parameter and to sustain it for a long time.

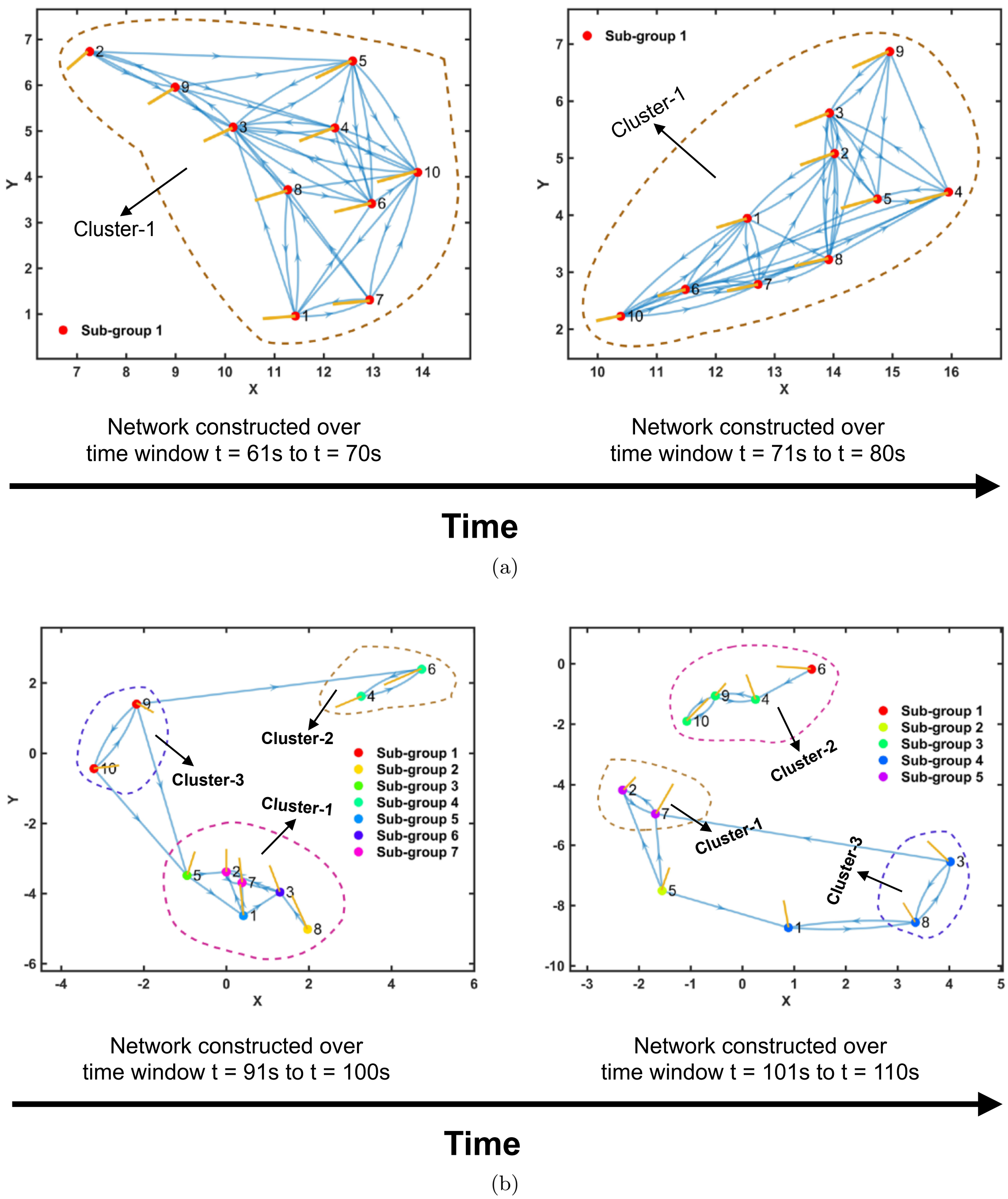

Figure 9: Clusters and sub-groups formed during collective motion are shown for two sets of snapshots of the simulation. Directed networks based on attraction interaction are constructed over a time window $t_w = 10\ s$, represented by blue arrows. The circular dots and orange arrows represent the heading of the organisms. Agents belonging to the same sub-group are marked with the same colour. Agents belonging to the same cluster are marked by dotted convex hulls. (a) - Network is constructed for $K = 3$, $r_a = 0.5\ \mathrm{s}^{-1}$, $r_p = 1\ \mathrm{s}^{-1}$ and $r_s = 1\ \mathrm{s}^{-1}$. The network is dense, hence the group is cohesive. (b) Network is constructed for $K = 1$, $r_a = 0.5\ \mathrm{s}^{-1}$, $r_p = 1\ \mathrm{s}^{-1}$ and $r_s = 1\ \mathrm{s}^{-1}$. Network is sparse, the clusters break apart often, as observed in the consecutive snapshots. Note here that the number of sub-groups are greater than the number of clusters.

References

Couzin, Iain D. et al. (2002). "Collective memory and spatial sorting in animal groups". In: *Journal of Theoretical Biology* 218.1, pp. 1–11. ISSN: 00225193. DOI: 10.1006/jtbi.2002.3065.

Gillespie, Daniel T. (1976). "A general method for numerically simulating the stochastic time evolution of coupled chemical reactions". In: *Journal of Computational Physics* 22.4, pp. 403–434. ISSN: 10902716. DOI: 10.1016/0021-9991(76)90041-3.

— (1977). "Exact stochastic simulation of coupled chemical reactions". In: *Journal of Physical Chemistry* 81.25, pp. 2340–2361. ISSN: 00223654. DOI: 10.1021/j100540a008.

Hemelrijk, Charlotte K. and Hanno Hildenbrandt (2008). "Self-organized shape and frontal density of fish schools". In: *Ethology* 114.3, pp. 245–254. ISSN: 01791613. DOI: 10.1111/j.1439-0310.2007.01459.x.

Hemelrijk, Charlotte K. and Hanspeter Kunz (2005). "Density distribution and size sorting in fish schools: An individual-based model". In: *Behavioral Ecology* 16.1, pp. 178–187. ISSN: 10452249. DOI: 10.1093/beheco/arh149.

Herbert-Read, James E. et al. (2011). "Inferring the rules of interaction of shoaling fish". In: *Proceedings of the National Academy of Sciences of the United States of America* 108.46, pp. 18726–18731. ISSN: 00278424. DOI: 10.1073/pnas.1109355108.

Huth, Andreas and Christian Wissel (1992). "The simulation of the movement of fish schools". In: *Journal of Theoretical Biology* 156.3, pp. 365–385. ISSN: 10958541. DOI: 10.1016/S0022-5193(05)80681-2.

— (1994). "The simulation of fish schools in comparison with experimental data". In: *Ecological Modelling* 75-76.C, pp. 135–146. ISSN: 03043800. DOI: 10.1016/0304-3800(94)90013-2.

Jhawar, Jitesh et al. (2020). "Noise-induced schooling of fish". In: *Nature Physics* 16.4, pp. 488–493. ISSN: 17452481. DOI: 10.1038/s41567-020-0787-y. URL: http://dx.doi.org/10.1038/s41567-020-0787-y.

Katz, Yael et al. (2011). "Inferring the structure and dynamics of interactions in schooling fish". In: *Proceedings of the National Academy of Sciences of the United States of America* 108.46, pp. 18720–18725. ISSN: 00278424. DOI: 10.1073/pnas.1107583108.

Lei, Liu et al. (2020). *Computational and robotic modeling reveal parsimonious combinations of interactions between individuals in schooling fish.* Vol. 16. 3, pp. 1–45. ISBN: 1111111111. DOI: 10.1371/journal.pcbi.1007194.

Strömbom, Daniel et al. (2019). "Asynchrony induces polarization in attraction-based models of collective motion". In: *Royal Society Open Science* 6.4. ISSN: 20545703. DOI: 10.1098/rsos.190381.